ENERGY AND RESOURCE SAVING / ЭНЕРГО- И РЕСУРСОСБЕРЕЖЕНИЕ

UDC 66-9
https://doi.org/10.17073/0021-3438-2025-1-80-90

Research article
Научная статья

Enhancing efficiency and modeling the operation of the afterburning chamber in the Vanyukov furnace

V.A. Kirsanov[1], **Yu.F. Poberezhny**[1], **N.G. Mikhailov**[1], **M.M. Sladkov**[2], **S.N. Gotenko**[2]

[1] **Ural Research and Design Institute of Mining Processing, Metallurgy, Chemistry, Standartization**
87 Khokhryakov Str., Ekaterinburg 620063, Russia

[2] **Sredneuralsky Copper Smeltery**
1 Sredneuralskaya Str., Revda 623280, Russia

✉ Nikolai G. Mikhailov (Mikhaylov_NG@umbr.ru)

Abstract: This study investigates the process of enhancing the efficiency of the afterburning chamber in the Vanyukov furnace. Various operational modes of the furnace and the chamber were analyzed to identify optimal conditions for sulfur oxidation and afterburning, as well as methods for reducing accretions. Measurements and analyses of off-gas compositions were conducted, and the dust content was determined. Simplifications and assumptions were applied in the calculations, enabling the modeling of gas flow, thermodynamic processes, velocity profiles, and interaction zones. Some thermodynamic calculations of counter-penetrating gas jets were based on hypotheses derived from heat exchange theories in mixing devices. Experimental results of numerical modeling and predictive simulations within the afterburning chamber are presented. Parameters were measured, and aerodynamic characteristics of the tuyeres were charted at an average oxygen supply to the chamber of no more than 2500 n.m^3/h (38 n.m^3 per ton of batch load). Recommendations for effective technological operations were proposed. The expertise of specialists from the Sredneuralsk Copper Smelter, along with the results of trials and process modeling, facilitated the selection of the optimal tuyere air distribution. The findings reveal the complexity of aerodynamic and thermodynamic processes occurring within the afterburning chamber. These include interactions between tuyere cooling airflows, heat release from exothermic oxidation reactions, and forced and natural convection of off-gases with varying temperature gradients, all visualized within a single projection.

Keywords: afterburning chamber, improving efficiency, modeling, Vanyukov process.

For citation: Kirsanov V.A., Poberezhny Yu.F., Mikhailov N.G., Sladkov M.M., Gotenko S.N. Enhancing efficiency and modeling the operation of the afterburning chamber in the Vanyukov furnace. *Izvestiya. Non-Ferrous Metallurgy.* 2025;31(1):80–90.
https://doi.org/10.17073/0021-3438-2025-1-80-90

Повышение эффективности и моделирование использования камеры дожигания в печи Ванюкова

В.А. Кирсанов[1], **Ю.Ф. Побережный**[1], **Н.Г. Михайлов**[1], **М.М. Сладков**[2], **С.Н. Готенко**[2]

[1] **Уральский научно-исследовательский и проектный институт обогащения и механической обработки полезных ископаемых**
Россия, 620063, Свердловская обл., г. Екатеринбург, ул. Хохрякова, 87

[2] **Среднеуральский медеплавильный завод**
Россия, 623280, Свердловская обл., г. Ревда, ул. Среднеуральская, 1

✉ Николай Григорьевич Михайлов (Mikhaylov_NG@umbr.ru)

Аннотация: В исследуемом процессе повышения эффективности использования камеры дожигания в печи Ванюкова изучены различные эксплуатационные варианты работы печи и камеры, найдены режимы оптимального окисления и дожигания серы, выявлены способы снижения настылеобразования. Проведены измерения и анализ отходящих газов. Определен состав пыли.

По результатам выполненных расчетов применяли ряд упрощений и допущений, позволяющих представлять движение газов, термодинамические процессы, профиль скоростей, области взаимодействия. Некоторые варианты термодинамических расчетов взаимопроникающих встречных струй построены на гипотезах, заимствованных из теории теплообмена в смешивающих аппаратах. Представлены экспериментальные результаты численного моделирования и варианты некоторых прогнозных симуляций, происходящих в камере дожигания печи Ванюкова. Проведены замеры параметров, построены графики аэродинамических характеристик фурм при среднем значении подачи кислорода в пространство камеры дожигания не более 2500 н.м^3/ч (38 н.м^3/т загрузки шихты). Предложены мероприятия для эффективной технологической эксплуатации. Опыт специалистов Среднеуральского медеплавильного завода, результаты испытаний и моделирования процесса способствовали выбору наилучшего распределения дутья по фурмам. Полученные результаты свидетельствуют о достаточно сложных аэродинамических и термодинамических процессах, происходящих в пространстве камеры дожигания, представлении в одной проекции взаимодействий явлений динамики фурменных дутьевых потоков охлаждения, выделения тепловой энергии экзотермических реакций окисления, принудительной и естественной конвекции отходящих расплавных газов с различными температурными градиентами.

Ключевые слова: камера дожигания, повышение эффективности, моделирование, процесс Ванюкова.

Для цитирования: Кирсанов В.А., Побережный Ю.Ф., Михайлов Н.Г., Сладков М.М., Готенко С.Н. Повышение эффективности и моделирование использования камеры дожигания в печи Ванюкова. *Известия вузов. Цветная металлургия*. 2025;31(1):80–90. https://doi.org/10.17073/0021-3438-2025-1-80-90

Introduction

The domestic smelting technology — known as the Vanyukov process, employed for processing sulfide-copper concentrates — has several advantages over foreign analogs, including high specific productivity, process flexibility, simplicity and reliability of the metallurgical unit, and low capital and operating costs. The smelting technology, in general, can be characterized as a semi-autogenous process [1—3].

During the testing period, the charge materials composition was as follows (wt. %): Cu — 17.97, S — 26.16, SiO — 15.28, Zn — 1.75, Pb — 0.25, others — 38.59.

In the horizontal section, the furnace consists of smelting-oxidation and sedimentation zones, while in the vertical section, it is divided into superstratum, supra-tuyere, and sub-tuyere zones. The furnace, in cross-section, is a rectangular-trapezoidal unit into which the blast is introduced through tuyeres. Charge materials are fed into the working space of the unit via loading devices. During the first stage of processing, heating, oxidation, and melting of the charge materials dominate [4]. The process characteristics are heavily influenced by the chemical, mineralogical, and granulometric composition of the ore [5]. In the supra-tuyere zone, processes such as melting, dissolution of refractory components, sulfide oxidation, and the coalescence of matte droplets take place [6—8]. Oxidation of off-gases occurs in the afterburning chamber, which is equipped with four tuyeres.

The issues related to improving efficiency and the simulation and optimization of the afterburning chamber's operation in the Vanyukov furnace will be examined in detail, as enhancing operational energy efficiency holds both practical and theoretical significance [9].

Research methodology

The methodology for determining the optimal modes of blast supply to the tuyere row of the afterburning chamber and optimizing the sulfur afterburning process was divided into practical and methodological components, with elements of visual representation.

In the methodological component, based on the results of the calculations, a number of simplifications and assumptions were applied to model gas flow, velocity profiles [10], thermal processes, and surface interaction zones. Some thermodynamic calculations of interpenetrating counter jets were built on concepts borrowed from the theory of heat exchange in mixing devices [11; 12]. For the numerical theoretical aspects of modeling hydrodynamic characteristics, the following formulas were used:

$$W_2 = [0.5gh^{-1}Ld^{-1}\gamma_0\mu(1 + \beta t)]^{0.5}, \quad (1)$$

$$\mathrm{Re} = Wd_t/\nu, \quad (2)$$

where γ_0 — specific mass of the gas; β — coefficient of volumetric gas expansion; L — space length; d — space diameter; h — geometric head; g — gravitational acceleration; μ — friction coefficient; t — temperature; ν — viscosity coefficient; W — blast velocity; W_2 — gas flow velocity; d_t — tuyere outlet diameter; Re — Reynolds number (dimensionless coefficient).

During the numerical modeling of heat release in the afterburning chamber, combustion reactions of sulfur and sulfur dioxide were considered:

$$S + O_2 = SO_2 + 297\ \mathrm{kJ}, \quad (3)$$

$$2SO_2 + O_2 = 2SO_3 + 192\ \mathrm{kJ}. \quad (4)$$

To analyze the thermal processes in the studied O_{xyz} space, the area of off-gas flow, A, was divided into grid

sections ΔN_1, ΔN_2, ..., ΔN_n with volumes ΔV_1, ΔV_2, ..., ΔV_n. The integral sum for the function $f(x,y,z)$ over area A is given by

$$M_n = \sum f(x_j, y_j, z_j)\Delta V_j. \quad (5)$$

The volumetric region of heat release from the jet streams was determined as:

$$\int dx \int dy \int f(x,y,z)dz, \quad (6)$$

$$a \le x \le b,\ c \le y \le e,\ m \le z \le n. \quad (7)$$

For each operational mode, technological data were monitored, and the composition of the off-gases was determined. Based on the balance indicators, the afterburning efficiency was evaluated (Table 1).

Table 1 includes the following parameters: S_a — amount of sulfur dioxide after the afterburning chamber; S_v — sulfur content in dust; S_{sh} — sulfur content in the charge materials; K_v — oxygen concentration in the off-gases exiting the afterburning chamber; K_d — oxygen supplied to the afterburning chamber.

To determine afterburning efficiency, the oxygen and gas blast parameters at the furnace's tuyere rows were recorded. Oxygen was supplied for afterburning at a rate not exceeding 2500 n.m^3/h (38 n.m^3 per ton of charge). Operating parameters were determined using measurement instrument readings. For comprehensive analysis, data from the information system's hourly and shift reports on furnace performance were used. Information on the composition of matte, slag, and dust was considered, and the composition of off-gases was analyzed.

Table. 1. **Combustion efficiency assessment**

Таблица 1. Оценка полноты сжигания

Mode	S_{sh}	S_a	S_v	K_v	K_d	Effect
Baseline	const	↕	↕	↕	↕	
1	const	↑	↓	↑	↑	+
2	const	↓	↑	↓	↓	–
3	const	↑	↓	↕	↕	+
4	const	↓	↑	↑	↕	–

Note. ↑ – increase, ↓ – decrease, ↕ – baseline values, «+» or «–» – indicates the afterburning efficiency achieved.

Results and discussion

In the studied gas flow process, the operational features of the afterburning chamber and the dynamic effects of jets emerging from the furnace tuyeres were examined, despite the presence of thermal and gas-dynamic inhomogeneities. Various operational modes of the furnace and afterburning chamber were analyzed, leading to the identification of optimal oxidation regimes and methods for enhancing the efficiency of accretion reduction. Schematic of the tuyere row is presented in Fig. 1.

During the tests, the oxygen pressure at the tuyere was regulated using shut-off and control valves, with the pressure readings recorded on the installed manometer, as well as the flow rate monitored via the information system. The resulting characteristics are presented in Fig. 2 and Table 2.

The provided tuyere characteristics enable individual regulation of the oxygen flow rate through each tuyere in varying proportions, while maintaining an approximate overall oxygen supply to the afterburning chamber depending on the furnace load.

A more detailed examination of the blast supply through the tuyeres of the afterburning chamber reveals that, due to turbulence, the free jet mixes with the surrounding medium as it moves away from the source. Free boundary layer forms within the jet, expanding

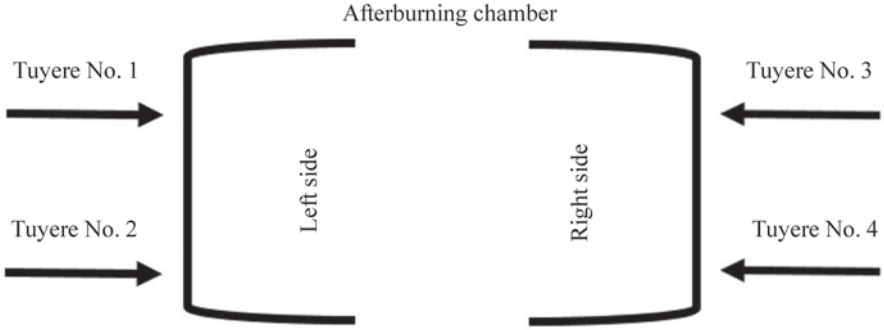

Fig. 1. Afterburning chamber tuyeres

Рис. 1. Фурмы камеры дожигания

Table. 2. **Calculated blast velocity modes**

Таблица 2. Расчетные скорости дутьевых режимов

Right side of the afterburning chamber						Left side of the afterburning chamber					
Tuyere *1*			Tuyere *2*			Tuyere *3*			Tuyere *4*		
W, m/s	Re, 10^4		*W*, m/s	Re, 10^4		*W*, m/s	Re, 10^4		*W*, m/s	Re, 10^4	
102.1	26–67	min	93.8	24–60	min	74.1	19–60	min	81.66	21–61	min
124.3			105.9			93.8			102.83		
142.2			118.0			110.4			115.69		
155.0			133.1			128.5			134.59		
166.3			143.7			139.1			146.69		
189.0		max	163.3		max	158.8		max	166.35		max
211.7			181.5			177.7			181.47		
242.7			196.6			196.6			201.13		
264.6			219.3			214.7			219.27		
			235.9			234.4			240.45		

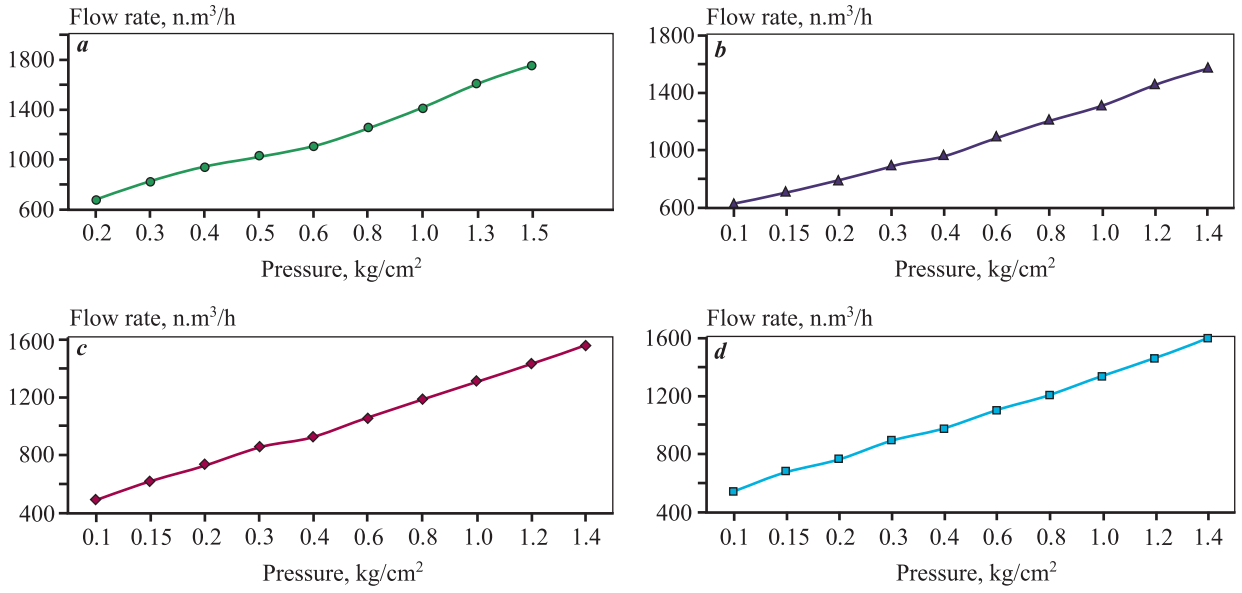

Fig. 2. Oxygen flow rate as a function of pressure

a – left side of the afterburning chamber, tuyere *1*; ***b*** – left side of the afterburning chamber, tuyere *2*;
c – right side of the afterburning chamber, tuyere *3*; ***d*** – right side of the afterburning chamber, tuyere *4*

Рис. 2. Зависимости расхода кислорода от давления

a – левая сторона камеры дожигания, фурма *1*; ***b*** – левая сторона камеры дожигания, фурма *2*;
c – правая сторона камеры дожигания, фурма *3*; ***d*** – правая сторона камеры дожигания, фурма *4*

outward from the nozzle, with primary mixing beginning at this boundary. This velocity adjustment within the jet leads to the formation of vortex regions in the cross-sectional plane. In other words, the most active interaction area is the collision point of the jets. This is because the velocities of the opposing jets are similar, causing the laminar flow zone to transition into turbulence [13—15]. Fig. 3 illustrates the vortex collision structures at relatively similar velocities of the opposing jets.

Due to the characteristics of off-gas flow and the non-uniformity caused by the connection of the furnace's tuyere rows and its geometry, jet flow modeling in the afterburning chamber represents a specific case [16—26].

The concentration of thermal energy in the jet interaction zones was calculated for both sulfur oxidation and

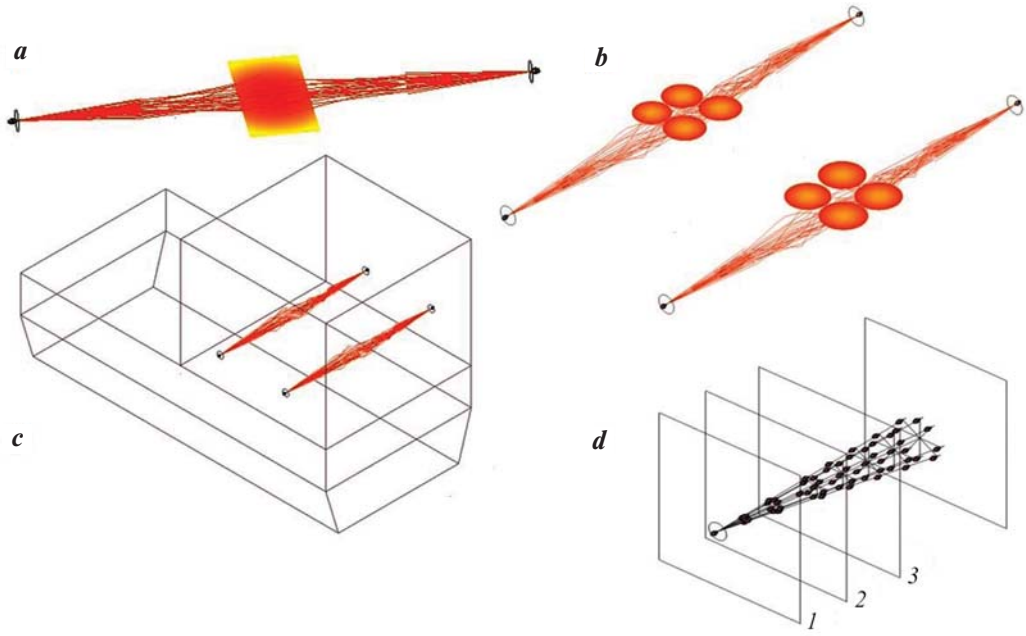

Fig. 3. Vortex collision structures

a – thermal zone of vortex collision; ***b*** – thermal structure of vortex collision; ***c*** – free turbulent jets in the afterburning chamber space; ***d*** – sections of a free turbulent jet: laminar (***1***), transitional (***2***), fully turbulent (***3***)

Рис. 3. Структуры вихревого соударения

a – термическая область вихревого соударения; ***b***– термическая структура вихревого соударения; ***c*** – свободные турбулентные струи в пространстве камеры дожигания; ***d*** – участки свободной турбулентной струи: ламинарный (***1***), переходной (***2***) и свободный турбулентный (***3***)

natural gas combustion processes. It was assumed that the Mach number for jets during sulfur oxidation does not exceed 0.52.

The calculated surface areas were determined for the jet collision zones and the jet flow regions. Within the boundaries of the interaction zone, a geometric figure was constructed with its axis aligned to the axis of the analyzed regions. Using polynomial distribution, it was assumed that a certain amount of sulfur is probabilistically combusted within the surface interaction zone.

As a result, the following volumetric heat loads were obtained: 500—1500 kW for oxidation processes and 1100—2200 kW for natural gas combustion. The normative heat load values for these processes were applied to the volumetric space of the afterburning chamber, while the actual heat load was determined based on the constructed surface interaction zones. The results are summarized in Table 3.

Examples of gas flow and jet stream are shown in Fig. 4.

The three-dimensional representation of the gas flows in the furnace reveals a variety of circulation zones. Velocity adjustments lead to the dominant jet, with the highest momentum and exit velocity, restructuring the opposing jet. This results in displacement starting from the turbulent boundary layer, causing jet separation. The flows enveloping the restructured jet acquire turbulent properties and a lower velocity, vectorially directed toward the boundaries of the afterburning chamber space. Considering the dynamics of opposing jets, it can be concluded that changes in velocity characteristics not only alter the thermal interaction zone but also influence the exhaust gas flow. It has been established that the structure of the collision zone depends on the design and operational parameters of the jet flow's swirl [26, 27]. Understanding the behavior of opposing colliding jets can be utilized for cleaning and preventing active accretion formation, as well as optimizing sulfur

Table. 3. **Assessment of thermal energy concentrations**

Таблица 3. Оценка концентраций тепловой энергии

Process	Heat load, kW/m^3		Local heat load coefficient [26]
	Normative	Actual	
Sulfur oxidation	40	1500	37
Natural gas combustion	65	2200	34

oxidation processes. The parameters of the off-gas are presented in Table 4.

Observations indicate that the rate of tuyere fouling depends on the external environment, blast pressure, as well as the direction and composition of the particles in the exhaust gases. Dust samples were collected from several points along the gas duct: waste heat boiler, cooling tower, and electrostatic precipitator. The results of the dust composition analysis are shown in Table 5.

Comparative analysis of sulfur content in dust and charge under different operating modes of the afterburning chamber is presented in Fig. 5.

The tests revealed that sulfur afterburning regulation can be performed both quantitatively and qualitatively. Increasing oxygen supply to the afterburning chamber, up to certain limits, raises the sulfur dioxide concentration in the off-gas and reduces the sulfur mass fraction in the dust.

Using computer modeling, various cases of accretion formation on one of the afterburning chamber walls were visualized is presented in Fig. 6.

The illustrated accretion formation variants, which occur during operation as a result of dust particle sintering in the off-gas, affect the performance of the blast tuyeres. Tuyere fouling is detected either by changes in blast pressure, during tuyere cleaning, or visually through open "inspection windows".

During operation, spontaneous tuyere cleaning may

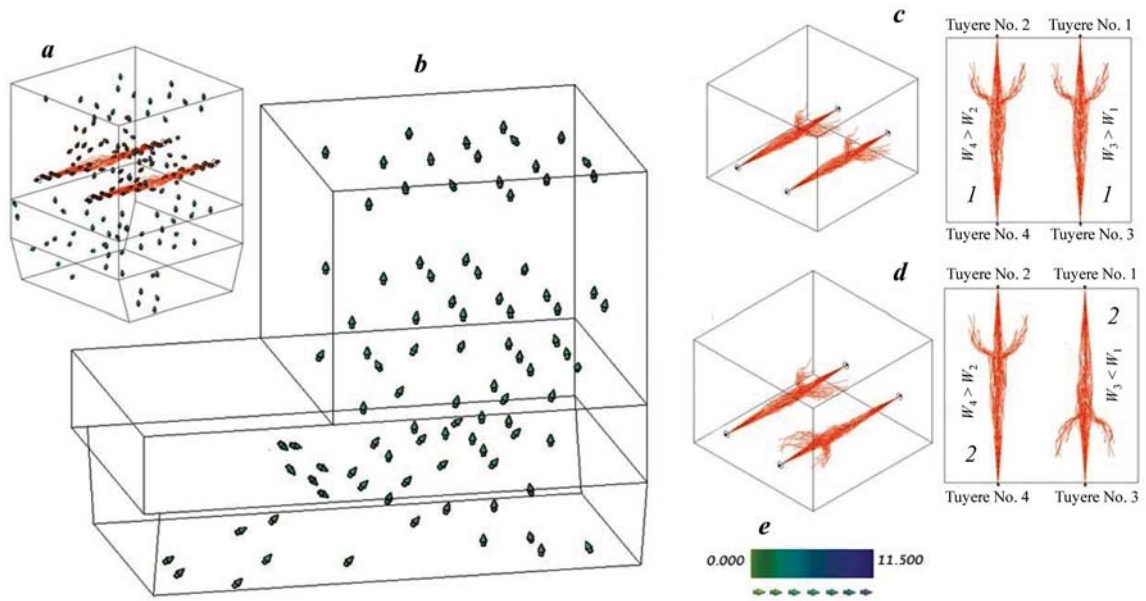

Fig. 4. Gas flow and jet stream

a – jet streams and off-gas flow; ***b*** – flow of high-temperature gases; ***c***, ***d*** – formation of collision structures at different jet velocities: ***1***, ***2*** – variations in jet velocity; ***e*** – velocity scale of high-temperature gases (m/s)

Рис. 4. Движение газов и струйный поток

a – струйный поток и движение уходящих газов; ***b*** – движение расплавных газов; ***c***, ***d*** – формирование структур соударения на разных струйных скоростях: ***1***, ***2*** – варианты скоростных изменений струй; ***e*** – шкала скорости расплавных газов, м/с

Table. 4. **Off-gas parameters**

Таблица 4. Параметры отходящих газов

Gas component	Gas density, kg/n.m^3	Mass fraction, kg/kg	Volume fraction, n.m^3/n.m^3
N_2	1.25	0.0483	0.0746
CO	1.25	–	–
CO_2	1.963	0.0768	0.0755
SO_2	2.855	0.07087	0.479
H_2O	0.863	0.139	0.334
O_2	1.427	0.027	0.0365
Note. The off-gas temperature is 1250 °C.			

occur, with the accretion breaking off due to the jet's own pressure. Installing a gas burner in the tuyeres of the third row is currently the primary method of combating accretion formation in the working space of the afterburning chamber. Table 6 shows the changes in the working space volume of the afterburning chamber due to accretion formation.

The data in Table 6 demonstrate that the working space volume of the afterburning chamber can significantly decrease due to perimetric accretion formation. This reduction leads to changes in the particle flow trajectories of the off-gases, deviations in the dynamic resistance during gas removal, and a decline in sulfur oxidation efficiency.

To determine the most efficient operation of the afterburning chamber, including the optimal oxygen flow through its tuyeres, calculation schemes and gas flow ratios were developed and evaluated for several existing and prospective operating modes. The optimal mode for the current system was identified, meeting the requirements for optimal afterburning, improved chamber efficiency, and enhanced sulfur oxidation. The results of gas composition measurements under different operating modes are presented in Table 7.

The results in Table 7 indicate that the uniformity of optimal sulfur oxidation and afterburning depends on jet dynamics. Various design options for modernizing the afterburning chamber are proposed in Fig. 7. Additional simulations and studies are necessary to confirm the effectiveness of these modernizations.

Conclusion

The findings highlight the complexity of the aerodynamic and thermodynamic processes within the afterburning chamber. The study employed turbulent jet theories and physical modeling. The blast supply was optimized for various experimental modes, with parameters measured and aerodynamic characteristics of the tuyeres charted at an average oxygen supply rate to the afterburning chamber of no more than 2500 n.m^3/h (38 n.m^3 per ton of charge). Gas analyses were performed, and the dust composition was determined at several points along the gas duct, including the waste heat boiler, cooling tower, and electrostatic precipitator.

Several schemes for modernizing the afterburning chamber and optimizing tuyere blast distribution were proposed. It was determined that the highest sulfur afterburning efficiency can be achieved by supplying a specific oxygen flow rate to each tuyere without altering the overall oxygen supply.

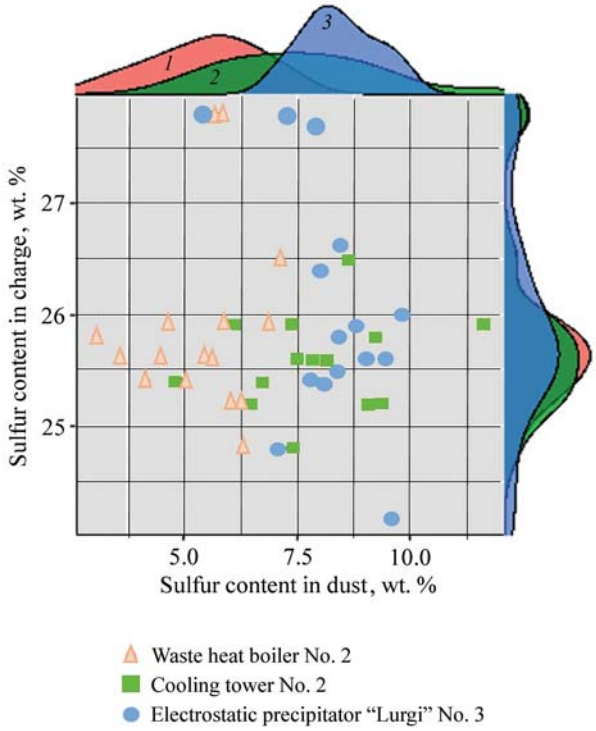

Fig. 5. Sulfur content in dust and charge under different operating modes of the afterburning chamber

1–3 – sulfur content density distribution assessment
1 – waste heat boiler No. 2; ***2*** – cooling tower No. 2;
3 – electrostatic precipitator "Lurgi" No. 3

Рис. 5. Содержание серы в пыли и шихте на разных режимах работы камеры дожигания

1–3 – оценка плотности распределения содержания серы
1 – котел-утилизатор № 2; ***2*** – башня охлаждения № 2;
3 – электрофильтр «Lurgi» № 3

Table. 5. **Dust composition, wt. %**

Таблица 5. Состав пыли, мас. %

Sampling point	Cu	S	Pb	Zn	Others
Cooling tower No. 2	19.45	5.45	3.69	3.28	68.13
Waste heat boiler No. 2	18.78	7.61	4.29	3.31	66.01
Electrostatic precipitator "Lurgi" No. 3	14.84	8.43	6.93	4.65	65.15

Table. 6. **Perimetric formation**

Таблица 6. Периметральное образование настыли

Variant	Working space volume, m^3	Thickness of wall accretion, m
1	55–59	0.1–0.2
2	49–53	0.25–0.35
3	37.5–43.0	0.50–0.65
4	34.0–37.6	0.65–0.75

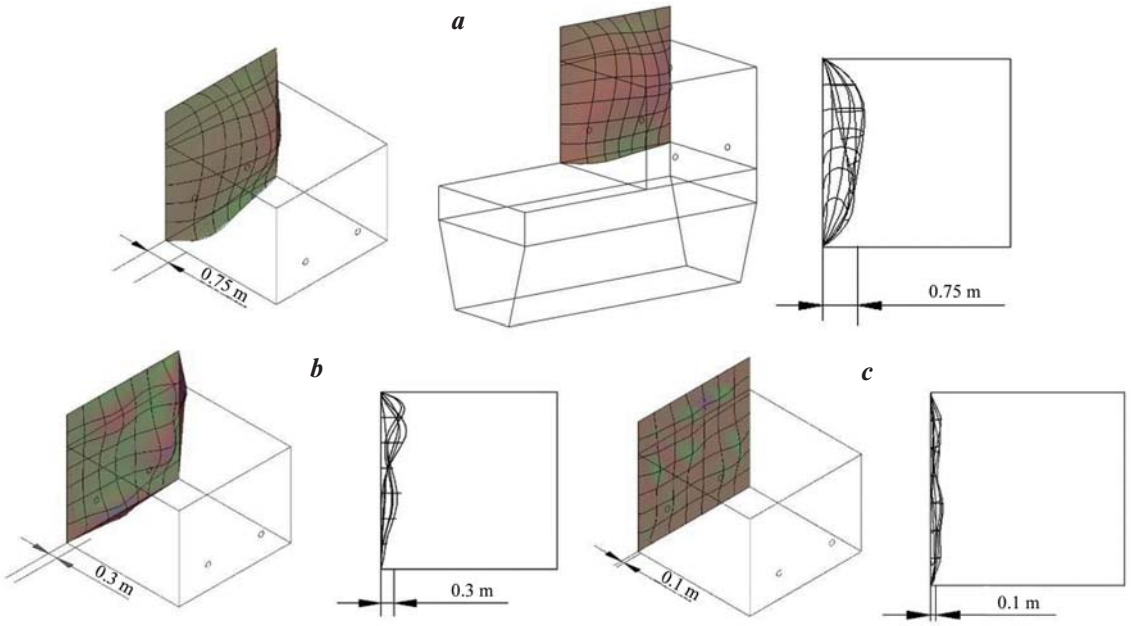

Fig. 6. Variants of accretion formation
Accretion thickness, m: ***a*** – 0.75; ***b*** – 0.3; ***c*** – 0.1

Рис. 6. Варианты настылеобразования
Толщина настыли, м: ***a*** – 0,75; ***b*** – 0,3; ***c*** – 0,1

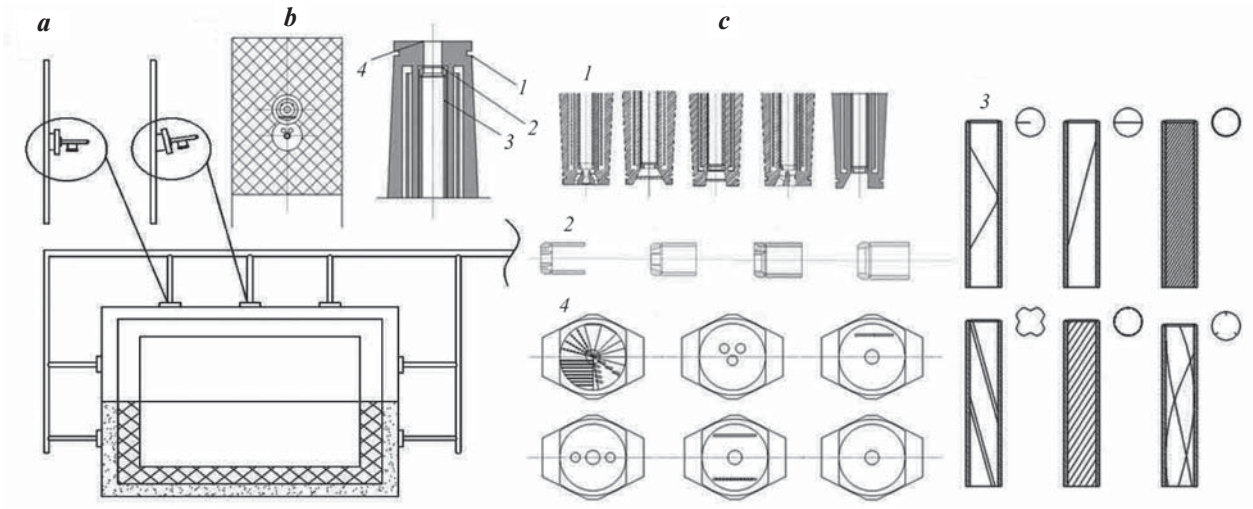

Fig. 7. Prospective options for modernizing the afterburning chamber [27–30]
a –arrangement of tuyeres in the afterburning chamber; ***b*** – multi-channel tuyere with two tiers of nozzles; ***c*** – modernization options for tuyere components: casing (***1***), sleeve (***2***), swirl inserts (***3***), and diffuser (***4***)

Рис. 7. Перспективные варианты направлений модернизации камеры дожигания [27–30]
a – вариант расположения фурм в камере дожигания; ***b*** – многоканальная фурма с двумя ярусами сопел; ***c*** – на участке фурмы варианты модернизации корпуса (***1***), втулки (***2***), вставок-завихрителя (***3***), рассекателя (***4***)

Measures for efficient operation and minimizing accretion formation in the Vanyukov furnace afterburning chamber were proposed. To implement a prospective automated operation, it is recommended to organize information tracking for each tuyere (pressure/flow rate), install regulating valves to adjust the blast flow rate to each tuyere without manual intervention, and introduce an automatic control system [31].

The expected outcomes of implementing these measures and recommendations include improved energy efficiency and operational safety, increased productivity, and enhanced control over the technological process.

Table. 7. **Off-gas composition measurements (wt.%) after afterburning in different operating modes of the afterburning chamber**

Таблица 7. Результаты измерений состава отходящих газов (мас. %) после дожигания на разных режимах эксплуатационной работы камеры дожигания

Measurement No.	First mode			Second mode		
	Oxygen supply to the afterburning chamber, $n.m^3/h$					
	2300			2500		
	SO_2	CO_2	O_2	SO_2	CO_2	O_2
1	38.0	10.4	4.0	42.4	11.0	4.5
2	40.0	10.0	4.5	41.0	10.5	4.5
3	38.0	10.4	4.6	42.0	11.0	4.5
4	39.8	10.9	4.5	42.4	11.6	5.0
5	38.4	10.4	4.7	43.0	12.0	5.0
	Average values					
	38.84	10.42	4.46	42.16	11.22	4.7

References

1. Lisienko V.G., Shchelokov Ya.M., Ladygichev M.G. Melting units: heat engineering, management and ecology. Moscow: Teplotekhnik, 2005. 912 p. (In Russ.).
Лисиенко В.Г., Щелоков Я.М., Ладыгичев М.Г. Плавильные агрегаты: теплотехника, управление и экология. М.: Теплотехник, 2005. 912 с.
2. Lisienko V.G., Shchelokov Ya.M., Ladygichev M.G. Fuel. Rational combustion, management and technological use. Moscow: Teplotekhnik, 2004. 832 p. (In Russ.).
Лисиенко В.Г., Щелоков Я.М., Ладыгичев М.Г. Топливо. Рациональное сжигание, управление и технологическое использование. М.: Теплотехник, 2004. 832 с.
3. Naboichenko S.S., Ageev N.G., Doroshkevich A.P., Zhukov V.P., Eliseev E.I. Processes and devices of non-ferrous metallurgy. Ekaterinburg: UGTU–UPI, 2005. 700 p. (In Russ.).
Набойченко С.С., Агеев Н.Г., Дорошкевич А.П., Жуков В.П., Елисеев Е.И. Процессы и аппараты цветной металлургии. Екатеринбург: УГТУ—УПИ, 2005. 700 с.
4. Sborshchikov G.S., Volodin A.M., Valavin V.S. Free convection of the melt in the furnace with a bubble layer during its blowing through a side tuyere established under the layer level. *Izvestiya. Non-Ferrous Metallurgy.* 2015;(2):58—68. (In Russ.).
Сборщиков Г.С., Володин А.М., Валавин В.С. Свободная конвекция расплава в печи с барботажным слоем при его продувке через боковую фурму, установленную под уровнем слоя. *Известия вузов. Цветная металлургия.* 2015;(2):58—68.
https://doi.org/10.17073/0021-3438-2015-2-58-68
5. Hoffman G.O. Metallurgy of copper. Sverdlovsk: GNTI, 1934. 475 p. (In Russ.).
Гофман Г.О. Металлургия меди. Свердловск: ГНТИ, 1934. 475 с.
6. Vanyukov A.V., Zaitsev V.Ya. Slags and matte of non–ferrous metallurgy. Moscow: Metallurgiya, 1969. 408 p. (In Russ.).
Ванюков А.В., Зайцев В.Я. Шлаки и штейны цветной металлургии. М.: Металлургия, 1969. 408 с.
7. Vaisburd S., Berner A., Brandon D.G., Kozhakhmetov S., Kenzhaliyev E., Zhalelev R. Slags & mattes in Vanyukov's process for the extraction of copper. *Metallurgical and Materials Transactions.* 2002;(33):551—559.
https://doi.org/10.1007/s11663-002-0034-1
8. Zhang H.L., Zhou C.Q., Bing W.U, Chen Y.M. Numerical simulation of multiphase flow in a Vanyukov furnace. *Journal of Southern African Institute of Mining and Metallurgy.* 2015;(115):457—463.
9. Anufriev V.P., Lisienko V.G., Chesnokov Yu.N., Lapteva A.V. Possibilities for implementing carbon policy in Russian regions. In: *Proceedings of the XII International conference «Russian regions in the focus of change»* (16–18 November 2017). Ekaterinburg: UMC UPI, 2018. Part 2. P. 536–550. (In Russ.).
Ануфриев В.П., Лисиенко В.Г., Чесноков Ю.Н., Лаптева А.В. Возможности реализации углеродной политики в российских регионах. В сб: *Материалы XII Международной конференции «Российские регионы в фокусе перемен»* (16—18 ноября 2017 г.). Екатеринбург: УМЦ УПИ, 2018. Ч. 2. С. 536—550.
10. Idelchik I.E. Handbook of hydraulic resistance. Moscow: Mashinostroenie, 1992. 672 p. (In Russ.).
Идельчик И.Е. Справочник по гидравлическим сопротивлениям. М.: Машиностроение, 1992. 672 с.
11. Kutateladze S.S. Fundamentals of the theory of heat transfer. Moscow: Atomizdat, 1979. 416 p. (In Russ.).
Кутателадзе С.С. Основы теории теплообмена. М.: Атомиздат, 1979. 416 с.
12. Baskakov A.P., Berg B.V., Vitt O.K., Filippovsky N.F. Teplotekhnika. Moscow: Energoatomizdat, 1991. 224 p. (In Russ.).
Баскаков А.П., Берг Б.В., Витт О.К., Филипповский Н.Ф. Теплотехника. М.: Энергоатомиздат, 1991. 224 с.

13. Abramovich G.N., Girshovich T.A., Krasheninnikov S.Yu., Secundov A.N., Smirnova I.P. Theory of turbulent jets. Moscow: Nauka, 1984. 710 p. (In Russ.).
Абрамович Г.Н., Гиршович Т.А., Крашенинников С.Ю., Секундов А.Н., Смирнова И.П. Теория турбулентных струй. М.: Наука, 1984. 710 с.
14. Colagrossi A., Marrone S., Colagrossi P., Le Touze D. Da Vinci's observation of turbulence: A French-Italian study aiming at numerically reproducing the physics behind one of his drawings, 500 years later. *Physics of Fluids*. 2021;(33):1—16. https://doi.org/10.1063/5.0070984
15. Prodanov S.A., Voronov G.V. Features of the movement of the gas medium in the above-tuyere zone of the Vanyukov furnace. In: *Materials of the V All-Russian scientific and practical conference of students, postgraduate students and young scientists* (12–13 May 2016). Ekaterinburg: UrFU, 2016. P. 91–98.
Проданов С.А., Воронов Г.В. Особенности движения газовой среды в надфурменной зоне печи Ванюкова. В сб. докл.: *Материалы V Всероссийской научно-практической конференции студентов, аспирантов и молодых ученых* (12—13 мая 2016 г.). Екатеринбург: УрФУ, 2016. С. 91—98.
16. Oliver T. Schmidt, Aaron Towne, Georgios Rigas, Tim Colonius, Guillaume A. Bres. Spectral analysis of jet turbulence. *Journal of Fluid Mechanics*. 2017;(855): 953—982. https://doi.org/10.1017/jfm.2018.675
17. Khansa Mahjoub Mohammed Merghani. Experimental study of a human-like exhaled airflow configuration and droplets dynamics in indoor environment. Paris: Universite Paris-EstCreteilVal-de-Marne, 2021. 183 p. https://theses.hal.science/tel-04022879
18. Barois T., Viggiano B., Basset T., Cal R.B., Volk R. Compensation of seeding bias for particle tracking velocimetry in turbulent flows. *Physical Review Fluids*. 2023;(8):1—16. https://doi.org/10.1103/PhysRevFluids.8.074603
19. Viggiano B., Basset T., Bourgoin M., Cal R.B., Chevillard L., Meneveau Ch., Volk R. Lagrangian modeling of a nonhomogeneous turbulent shear flow: Molding homogeneous and isotropic trajectories into a jet. *Physical Review Fluids*. 2024;(9):1—13.
https://doi.org/10.1103/PhysRevFluids.9.044604
20. Xinchen Zhang, Zhen Zhang, Alfonso Chinnici, Zhiwei Sun, Javen Qinfeng Shi, Graham J. Nathan, Rey C. Chin. Physics-informed data-driven unsteady Reynolds-averaged Navier—Stokes turbulence modeling for particle-laden jet flows. *Physical Review Fluids*. 2024;(36):1—23. https://doi.org/10.1063/5.0206090
21. Timothy C.W. Lau, Graham J. Nathan. Inuence of Stokes number on the velocity and concentration distributions in particle-laden jets. *Journal of Fluid Mechanics*. 2014;(757):432—457.
https://doi.org/10.1017/jfm.2014.496
22. Aitor Amatriain, Corrado Gargiulo, Gonzalo Rubio. Generalized wall-modeled large eddy simulation model for industrial applications. *Physics of Fluids*. 2024;(36): 1—21. https://doi.org/10.1063/5.0180690
23. Jonathan B. Freund. Nozzles, turbulence, and jet noise prediction. *Journal of Fluid Mechanics*. 2019;(860):1—4. https://doi.org/10.1017/jfm.2018.823
24. Muppidi S., Mahesh K., Direct numerical simulation of round turbulent jets in crossflow. *Journal of Fluid Mechanics*. 2007;(574):59—84.
https://doi.org/10.1017/S0022112006004034
25. Yu Zhou, Dewei Fan, Bingfu Zhang, Ruiying Li, Bernd R. Noack Artificial intelligence control of a turbulent jet. *Journal of Fluid Mechanics*. 2020;(897): 1—46. https://doi.org/10.1017/jfm.2020.392
26. Khudyakov P.Yu. Gas dynamics and heat transfer during collision of straight-flow gas jets: Abstract of the dissertation ... Cand. Sci. (Phys.-Math.). Ekaterinburg: UrFU, 2013. (In Russ.).
Худяков П.Ю. Газодинамика и теплообмен при соударении прямоточных газовых струй: Автореф. Дис. ... канд. физ.-мат. наук. Екатеринбург: УрФУ, 2013.
27. Phoebe Kuhn. Linear modeling of coherent structures in the self-similar region of a round turbulent jet: Diss. ... Dr. Eng. Berlin: Technischen Universität Berlin, 2023. https://doi.org/10.14279/depositonce-18798
28. Velkin V.I., Shkolny A.V., Kirillov M.P., Achkeev M.V., Gurin A.A. Swirler: Patent 2321779 (RF). 2006. (In Russ.).
Велькин В.И., Школьный А.В., Кириллов М.П., Ачкеев М.В., Гурин А.А. Завихритель: Патент 2321779 (РФ). 2006.
29. Francis B.J., Joubert H., Bakker M.L., Nikolic S., Gwynn-Jones S. Lance for use in a top submerged lance furnace. WO 2017/195105. 2017.
30. Shatokhin I.M., Kuzmin A.L. Method of circulating vacuuming of liquid metal, system and devices for its implementation: Patent 2213147 (RF). 2003. (In Russ.).
Шатохин И.М., Кузьмин А.Л. Способ циркуляционного вакуумирования жидкого металла, система и устройства для его осуществления: Патент 2213147 (РФ). 2003.
31. Zemtsov G.A., Puchkov A.E., Frolov L.I. Furma: Patent 2355779 (RF). 2009. (In Russ.).
Земцов Г.А., Пучков А.Е., Фролов Л.И. Фурма: Патент 2355779 (РФ). 2009.

Information about the authors

Vladimir A. Kirsanov – Advisor to the General Director for Engineering, Ural Research and Design Institute of Mining Processing, Metallurgy, Chemistry, Standartization (JSC "Uralmekhanobr").
E-mail: Kirsanov_VA@umbr.ru

Yuri F. Poberezhny – Head of the Bureau of Engineering and Innovation, JSC "Uralmekhanobr".
E-mail: Poberezhny_YF@umbr.ru

Nikolai G. Mikhailov – Leading Engineer of the Technological Audit Department, JSC "Uralmekhanobr".
https://orcid.org/0009-0006-2019-019X
E-mail: Mikhaylov_NG@umbr.ru

Maxim M. Sladkov – Chief Engineer of the Sredneuralsky Copper Smeltery (JSC "SUMZ").
E-mail: M.Sladkov@sumz.umn.ru

Sergey N. Gotenko – Head of the Technical Department, JSC "SUMZ".
E-mail: S.Gotenko@sumz.umn.ru

Информация об авторах

Владимир Андреевич Кирсанов – советник ген. директора по инжинирингу Уральского научного-исследовательского и проектного института обогащения и механической обработки полезных ископаемых (АО «Уралмеханобр»).
E-mail: Kirsanov_VA@umbr.ru

Юрий Федорович Побережный – начальник бюро инжиниринга и инноваций АО «Уралмеханобр».
E-mail: Poberezhny_YF@umbr.ru

Николай Григорьевич Михайлов – вед. инженер отдела технологического аудита АО «Уралмеханобр».
https://orcid.org/0009-0006-2019-019X
E-mail: Mikhaylov_NG@umbr.ru

Максим Михайлович Сладков – гл. инженер Среднеуральского медеплавильного завода (АО «СУМЗ»).
E-mail: M.Sladkov@sumz.umn.ru

Сергей Николаевич Готенко – начальник технического управления АО «СУМЗ».
E-mail: S.Gotenko@sumz.umn.ru

Contribution of the authors

V.A. Kirsanov – general supervision, editing of the article.

Yu.F. Poberezhny – participation in the discussion of results.

N.G. Mikhailov – data processing and preparation of the article.

M.M. Sladkov – resource support for the research.

S.N. Gotenko – resource support for the research.

Вклад авторов

В.А. Кирсанов – общее руководство, редактирование текста статьи.

Ю.Ф. Побережный – участие в обсуждении результатов.

Н.Г. Михайлов – обработка результатов исследования, подготовка статьи.

М.М. Сладков – ресурсное обеспечение исследования.

С.Н. Готенко– ресурсное обеспечение исследования.

The article was submitted 21.05.2024, revised 29.10.2024, accepted for publication 31.10.2024

Статья поступила в редакцию 21.05.2024, доработана 29.10.2024, подписана в печать 31.10.2024